Compressible Flows with Oscillating Boundaries

O. A. Logvinov

Moscow State University, Mechanics and Mathematics Department, Moscow, Russia
e-mail: oleglogvinov@mail.ru

Abstract—The flow of a viscous compressible heat-conducting fluid in a plane channel with rigid oscillating walls is considered. It is shown that even a vanishingly small compressibility can be the reason for the onset of a resonance, i.e., sharp increase in the amplitude of oscillations of the flow parameters at a properly selected wall oscillation frequency. An exact analytical expression for the leading resonant frequency is given. Numerical calculations have demonstrated the possibility of a cumulative effect, namely, sharp increase in the mass flow rate even at constant pressure gradient.

Flows in channels with moving boundaries are common in many technological natural and physiological processes. Various flows with oscillating solid parts arise in the aviation industry. A separate direction that has been successfully developing in our country for a long time is associated with the vibration effect on a deformable porous formation saturated with a fluid. In [1, 2], the solution for stationary oscillations of a two-phase "reservoir-liquid" system was obtained and the possibility of sharp increase in the amplitude of oscillations (resonance) at certain frequencies was shown for specific boundary conditions. It has been established that for all parameters the resonance corresponds to vibrations of the porous skeleton and fluid in one phase. It was shown that the resonance frequencies make it possible to create significant amplitudes at a great distance from the oscillation source.

The number of studies related in one or another way to problems with fully or partially movable boundaries is enormous. In the present brief review, we will focus only on some of them.

In [3], the flow of an incompressible viscous fluid in a plane channel or a cylindrical pipe with rigid walls moving along their normal was considered, so that the channel width or the pipe radius vary with time according to a given periodic law. In the case of a small amplitude of wall oscillations ε (referred to the width or radius of the channel), the solution was obtained at arbitrary vibrational Reynolds numbers α (the product of the Reynolds number and the Strouhal number) by expanding in series in ε. It is interesting that at low α the average velocities of individual particles are directed towards the walls, while at high α the drift occurs mainly from the walls. The particles that form a thin boundary layer represent an exception.

Also, in [3] the motion of the side channel walls, which occurs as a result of their elastic response to periodic pressures applied both at the ends of the channel and on the walls themselves, was studied. It turned out that the fluid-walls system has its own frequency. And if this frequency is a multiple of the frequency of external pressure oscillations, a resonance may occur. The proposed formulation has an application to the blood flow in the coronary arteries of large mammals.

In [4], the linear stability of the solution obtained in [3] was considered in the case of a plane channel. It was shown that an increase in the vibrational Reynolds number at sufficiently high amplitudes of wall vibrations leads to deterministic chaos according to the Feigenbaum scenario through a period doubling cascade.

In [5], a problem similar to [3] was considered but in the presence of gravity as well (the direction of flow formed an acute angle with the direction of gravity). It was shown that the high vibrational Reynolds numbers correspond to a drop in the flow rate, and not to its increase, as with low Reynolds numbers. The reason was that the time-average velocity field is composed of two components. The first component is determined only by wall vibrations and does not contribute to the average flow rate. The second component is associated with the combined action of three factors, namely, oscillations, gravity, and the pres-

sure drop. The distribution of the second component, depending on the longitudinal coordinate, has an extremum point in the middle of the channel: at low vibrational Reynolds numbers, this extremum turns out to be a maximum, for high ones it is a minimum.

In [6], gas oscillations that develop in a plane channel with excitation of the elastic walls of the channel symmetric with respect to the longitudinal axis were numerically simulated. The nature of resonant oscillations of the gas in the vicinity of the excitation region at various flow velocities was established.

The authors of [7] studied mass transfer in a plane channel with vibrating elastic walls. The solution was constructed by expansion in a small parameter ε. Not only vibrations in the form of traveling waves were considered, but also more general types of wall motions. It turned out that at high vibrational Reynolds numbers, standing waves give the maximum flow rate which is by an order of magnitude greater than the flow rate in the case of waves traveling along the elastic boundaries. Thus, the established opinion that traveling waves are the optimal mechanism for pumping fluid in a channel with vibrating deformable walls was refuted.

In [8], air flows in an oscillating cylindrical pipe were experimentally simulated. The frequencies of pressure oscillations in a "resting" pipe coincide with its natural frequencies. In the case of forced oscillations of the walls, the corresponding frequencies of pressure oscillations are the higher harmonics for the frequencies of the walls. In this case, the average pressure drops, and the maximum drop occurs in the center of the pipe. The flow rate also oscillates, but at much lower frequencies and with small amplitudes.

Concluding the review, we note that if the undisturbed flow velocity the is small as compared to the speed of sound in fluid (the Mach numbers are noticeably less than unity), the compressibility of fluid is almost always neglected. However, based on the linear theory, in [9] it was shown that in flows with fully or partially oscillating boundaries, even a vanishingly small compressibility can play the key role in the initiation of a resonance. In turn, numerical calculations demonstrated the possibility of a cumulative effect, namely, sharp increase in the mass flow rate even at constant pressure gradient.

The present study develops the ideas underlying [9]. The main difference is the consideration of the complete formulation of the problem with taking into account the energy equation and the thermodynamic equation of state for a perfect gas, while in [9] the fluid was considered to be weakly compressible. The motivation is to follow the changes in the temperature in the resonance regimes. The numerical simulation also takes into account changes in the viscosity and thermal conductivity along with changes in the temperature. However, these changes appear to be insignificant.

1. FORMULATION OF THE PROBLEM

We will consider flow of a *viscous compressible heat-conducting* liquid (gas) in a long plane channel with rigid walls. Some parts of the walls form vibrating sections capable of oscillating at a constant frequency ω in the direction perpendicular to the main flow (Fig. 1a). The amplitude of oscillations ε is small as compared to the channel width l. In Fig. 1b we have shown a separate section with the corresponding boundary conditions.

The flow is described by the two-dimensional Navier–Stokes equations in the Cartesian coordinates (x, y), the continuity equation, and the energy balance equation with the dynamic viscosity and thermal conductivity coefficients μ and θ that depend on the temperature T. The system is closed by the equations of state (thermodynamic and energy) of a perfect gas with constant heat capacities c_p and c_v

$$\frac{\partial \rho}{\partial t} + u\frac{\partial \rho}{\partial x} + \rho\frac{\partial u}{\partial x} + v\frac{\partial \rho}{\partial y} + \rho\frac{\partial v}{\partial y} = 0, \tag{1.1}$$

$$\rho\frac{Du}{Dt} + \frac{\partial p}{\partial x} = \frac{\partial}{\partial x}\left[\mu\left(2\frac{\partial u}{\partial x} - \frac{2}{3}\left(\frac{\partial u}{\partial x} + \frac{\partial v}{\partial y}\right)\right)\right] + \frac{\partial}{\partial y}\left[\mu\left(\frac{\partial u}{\partial y} + \frac{\partial v}{\partial x}\right)\right], \tag{1.2}$$

$$\rho\frac{Dv}{Dt} + \frac{\partial p}{\partial y} = \frac{\partial}{\partial x}\left[\mu\left(\frac{\partial u}{\partial y} + \frac{\partial v}{\partial x}\right)\right] + \frac{\partial}{\partial y}\left[\mu\left(2\frac{\partial v}{\partial y} - \frac{2}{3}\left(\frac{\partial u}{\partial x} + \frac{\partial v}{\partial y}\right)\right)\right], \tag{1.3}$$

$$\rho\frac{De}{Dt} + p\left(\frac{\partial u}{\partial x} + \frac{\partial v}{\partial y}\right) = \frac{\partial}{\partial x}\left(\theta\frac{\partial T}{\partial x}\right) + \frac{\partial}{\partial y}\left(\theta\frac{\partial T}{\partial y}\right) + \mu\,\Theta, \tag{1.4}$$
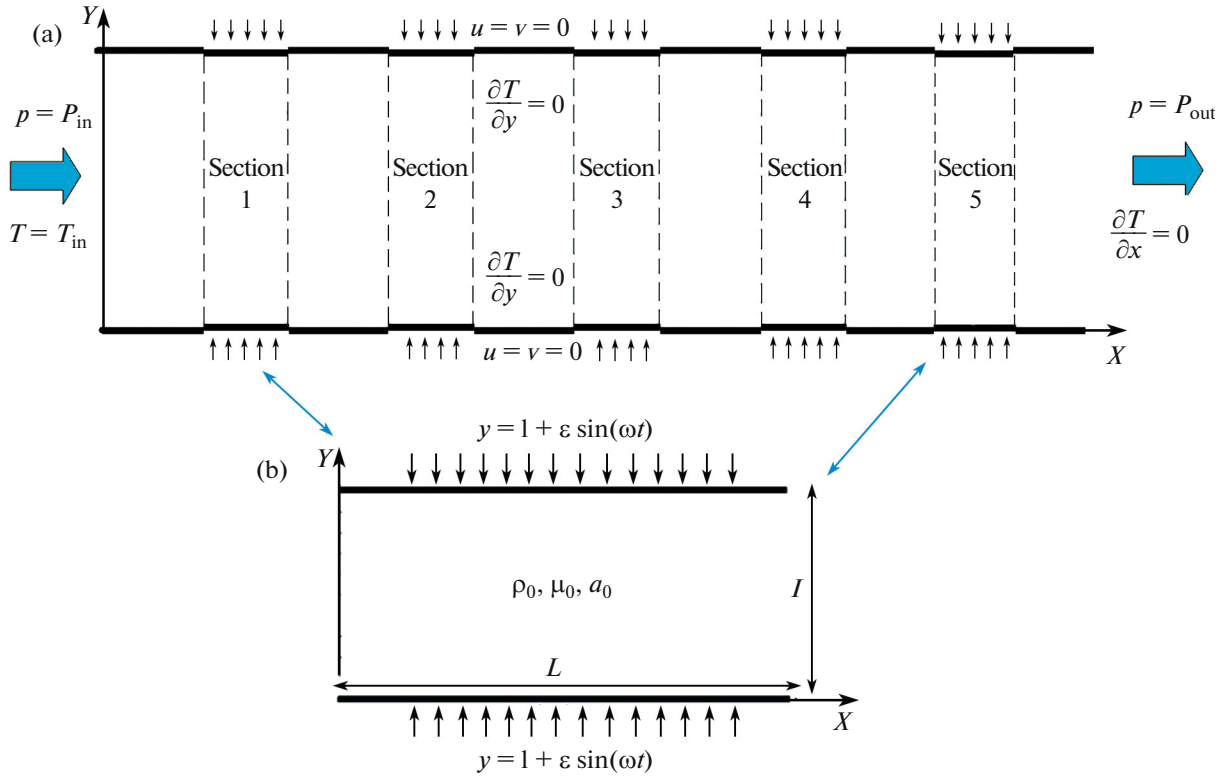
$$p = \rho RT, \quad e = c_v T, \tag{1.5}$$

Fig. 1. (a) Geometry of a plane channel with five oscillating wall sections; (b) separate oscillating section.

$$\mu = \mu_{contr} \frac{T_{contr} + T_\mu}{T + T_\mu} \left(\frac{T}{T_{contr}}\right)^{3/2}, \quad \theta = \theta_{contr} \frac{T_{contr} + T_\theta}{T + T_\theta} \left(\frac{T}{T_{contr}}\right)^{3/2}. \tag{1.6}$$

In system (1.1)−(1.6) we have adopted the following notation: u, v are the components of the velocity vector, p is the pressure, ρ is the density, T is the absolute temperature, e is the specific internal energy, $R = c_p − c_v$ is the gas constant, and Θ is the dissipation function:

$$\Theta = 2\left(\frac{\partial u}{\partial x}\right)^2 + 2\left(\frac{\partial v}{\partial y}\right)^2 + \left(\frac{\partial u}{\partial y} + \frac{\partial v}{\partial x}\right)^2 - \frac{2}{3}\left(\frac{\partial u}{\partial x} + \frac{\partial v}{\partial y}\right)^2.$$

Equations (1.2) and (1.3) are written within the framework of the Stokes hypothesis, namely, the volume (bulk) viscosity is assumed to be equal to zero: $\zeta^{vol} = \lambda + 2\mu/3 \equiv 0$, where λ is the second viscosity coefficient.

Formulas (1.6) are the Sutherland temperature dependences of the viscosity and thermal conductivity coefficients for a perfect gas, in which μ_{contr} and θ_{contr} are the reference viscosity and thermal conductivity at the reference temperature T_{contr}, and T_μ and T_θ are the Sutherland constants that characterize a particular gas.

System (1.1)−(1.6) must be supplemented with initial and boundary conditions. At the channel inlet, a constant inlet pressure and temperature must be set: $p = P_{in}$, $T = T_{in}$. At the channel outlet, we set a constant outlet pressure and a "soft" temperature condition: $p = P_{out}$, $\partial T/\partial x = 0$. On the vibrating sections of the channel walls, harmonic oscillations of the vertical velocity and the thermal insulation condition are set:

$$\{x \in \mathbf{X_{vibe}}, y = 0 + \varepsilon \sin(\omega t)\}: \quad u = 0, \quad v = V_d(t) = \varepsilon\omega\cos(\omega t), \quad \partial T/\partial y = 0, \tag{1.7a}$$

$$\{x \in \mathbf{X_{vibe}}, y = l + \varepsilon \sin(\omega t)\}: \quad u = 0, \quad v = V_u(t) = \varepsilon\omega\cos(\omega t), \quad \partial T/\partial y = 0. \tag{1.7b}$$

On the parts of the walls at rest, the usual no-slip and thermal insulation conditions are imposed. In conditions (1.7) $\mathbf{X_{vibe}}$ means the set of those $x \in [0; \Lambda]$ that correspond to the vibrating sections. Here and in what follows, Λ is the length of the entire channel and L is the length of a single section.

The initial conditions determine the state of rest

$$\{t = 0\}: \quad u = 0, \quad v = 0, \quad p = p_0, \quad T = T_0. \tag{1.8}$$

The closed mathematical model (1.1)−(1.8) forms the basis of this article, which consists of two parts. In the first part, linearized solutions for one oscillating section are analytically considered (Fig. 1b). In the second part, the nonlinear system (1.1)−(1.8) is solved by the finite-difference method in the complete channel geometry with five oscillating sections (Fig. 1a).

2. LINEARIZED SOLUTIONS

We will consider small perturbations of the initial state of rest in a simplified geometry, namely, for a single vibrating section (Fig. 1b). The main flow parameters will be denoted by the subscript zero and the perturbations will be denoted by primes.

From Eqs. (1.1)−(1.3) we can eliminate the velocity components:

$$\frac{\partial^2 \rho'}{\partial t^2} = \frac{a_0^2}{\gamma} \Delta \rho' + \rho_0 R \Delta T' + \frac{4}{3} \nu_0 \frac{\partial}{\partial t} \Delta \rho', \tag{2.1}$$

where $a_0^2 = \gamma R T_0$ is the undisturbed speed of sound, $\gamma = c_p/c_v$ is the specific heat ratio, and ν_0 is the undisturbed kinematic viscosity.

Then the equation (2.1) and the linearized equation (1.4) form a closed system for determining the density and temperature perturbations. The pressure perturbation is determined explicitly by the first (linearized) of Eqs. (1.5).

Eliminating the temperature from Eqs. (2.1) and (1.4), we can arrive at the following equation for the density (in what follows, primes will be omitted):

$$\frac{\partial}{\partial t}\left[\frac{\partial^2}{\partial t^2} - a_0^2 \Delta\right]\rho' - \Delta\left[\left(b_0^2 + \gamma c_0^2\right)\frac{\partial^2}{\partial t^2} - a_0^2 c_0^2 \Delta - \gamma b_0^2 c_0^2 \frac{\partial}{\partial t} \Delta\right]\rho' = 0 \tag{2.2}$$

where $b_0^2 = 4\nu_0/3$ and $c_0^2 = \theta_0/\rho_0 c_p$ is the fluid thermal diffusivity.

Note that in the absence of dissipative effects (viscosity and thermal conductivity), equation (2.2) reduces to the usual wave equation. Since the general solution of Eq. (2.2) is fairly cumbersome, it seems more clear to separate the study of the influence of dissipative effects: initially, we will consider a viscous but non-thermal-conducting fluid ($c_0^2 = 0$), and then an inviscid but heat-conducting one. Then, both results can be compared with the case of an ideal (inviscid and non-thermal-conducting) fluid. It can be shown that in both cases the temperature satisfies an equation completely analogous to Eq. (2.2) for the density.

We take the boundary conditions for Eq. (2.2) in the following form:

$$x = 0: \quad \rho = \rho_{in}, \quad x = L: \quad \rho = \rho_0, \tag{2.3a}$$

$$y = 0: \quad \rho = \rho_0\left[1 + (S/\rho_0)\sin(\omega t)\right], \quad y = l: \quad \rho = \rho_0\left[1 + (S/\rho_0)\sin(\omega t)\right], \tag{2.3b}$$

where S is a certain constant.

Note that the boundary conditions on the channel walls are linearized and "transferred" to their unperturbed position.

The initial conditions take the form:

$$t = 0: \quad \rho = \rho_0, \quad \partial \rho/\partial t = 0. \tag{2.4}$$

To solve Eq. (2.2), we will use the Fourier method of separation of variables. We will outline only the general scheme without computational details.

1. The boundary conditions (2.3b) in the y direction are set to zero by introducing the variable $\rho = \rho_0 + S \sin(\omega t) + \tilde{\rho}$. The variables are separated. The solution is decomposed into the eigenfunctions

$$\sin(\pi n y / l): \tilde{\rho} = \sum_{n=0}^{\infty} F_n(x,t) \sin \frac{\pi n y}{l}.$$

2. The boundary conditions (2.3a) in the x direction are set to zero by introducing the new variable $F_n = \tilde{F}_n - (\rho_{\text{in}} - \rho_0) c_n (x - L) / L - S c_n \sin(\omega t)$. The variables are separated. The solution is decomposed

into the eigenfunctions $\sin(\pi k x / L): \tilde{F}_n = \sum_{k=0}^{\infty} T_{nk}(t) \sin \frac{\pi k x}{L}.$

3. The problem is reduced to an ordinary differential equation for unknown functions of time $T_{nk}(t)$ with given initial conditions.

We present only the final equations. In the absence of heat conduction, the functions $T_{nk}(t)$ must satisfy the following ordinary differential equation:

$$\frac{d^2 T_{nk}}{dt^2} + 2\alpha_{nk} \frac{d T_{nk}}{dt} + \omega_{0nk}^2 T_{nk} = A'_{nk} \sin(\omega t) + B'_{nk} \cos(\omega t) + C'_{nk}, \tag{2.5a}$$

$$2\alpha_{nk} = b_0^2 \Omega_{nk}, \quad \omega_{0nk}^2 = a_0^2 \Omega_{nk}, \quad \Omega_{nk} = \left(\frac{\pi n}{l}\right)^2 + \left(\frac{\pi k}{L}\right)^2,$$

$$A'_{nk} = S \left(\frac{\pi n}{l}\right)^2 c_n d_k \frac{a_0^2}{\gamma}, \quad B'_{nk} = S \left(\frac{\pi n}{l}\right)^2 c_n d_k b_0^2 \omega, \quad C'_{nk} = \frac{a_0^2}{\gamma} \left(\frac{\pi n}{l}\right)^2 c_n e_k (\rho_{in} - \rho_0).$$

In the absence of viscosity, the equation for the functions $T_{nk}(t)$ takes the form:

$$\frac{d^3 T_{nk}}{dt^3} + \gamma \beta_{nk} \frac{d^2 T_{nk}}{dt^2} + \omega_{0nk}^2 \frac{d T_{nk}}{dt} + \beta_{nk} \omega_{0nk}^2 T_{nk} = A''_{nk} \sin(\omega t) + B''_{nk} \cos(\omega t) + C''_{nk}, \tag{2.5b}$$

$$\beta_{nk} = c_0^2 \Omega_{nk}, \quad \omega_{0nk}^2 = a_0^2 \Omega_{nk}, \quad A''_{nk} = S \left(\frac{\pi n}{l}\right)^2 c_n d_k c_0^2 \left(a_0^2 \left(\frac{\pi n}{l}\right)^2 - \gamma \omega^2\right),$$

$$B''_{nk} = S \left(\frac{\pi n}{l}\right)^2 c_n d_k a_0^2 \omega, \quad C''_{nk} = a_0^2 c_0^2 \left(\frac{\pi n}{l}\right)^4 c_n e_k (\rho_{in} - \rho_0).$$

The Fourier coefficients c_n, d_k, and e_k in Eqs. (2.5) can be determined from the relations

$$c_n = \frac{2}{\pi n}(1 - (-1)^n), \quad d_k = \frac{2}{\pi k}(1 - (-1)^k), \quad e_k = \frac{2}{\pi k}. \tag{2.6}$$

The initial conditions for Eqs. (2.5) take the form:

$$t = 0: \quad T_{nk} = (\rho_{in} - \rho_0) c_n e_k, \quad \frac{d T_{nk}}{dt} = 0. \tag{2.7}$$

The solution of the ordinary differential equation (2.5a), corresponding to the absence of heat conduction, is the sum of the general and particular solutions (2.8a) and (2.9a)

$$T_{nk,\text{vis}}^{\text{gen}}(t) = e^{-\alpha_{nk} t} [D'_{1nk} \sin(\sqrt{\omega_{0nk}^2 - \alpha_{nk}^2} t) + D'_{2nk} \cos(\sqrt{\omega_{0nk}^2 - \alpha_{nk}^2} t)], \tag{2.8a}$$

$$T_{nk,\text{vis}}^{\text{part}}(t) = \Psi'_{nk} \sin(\omega t + \theta'_{nk}) + \frac{C'_{nk}}{\omega_{0nk}^2}, \tag{2.9a}$$

$$\Psi'_{nk} = \frac{\sqrt{A'^2_{nk} + B'^2_{nk}}}{\sqrt{(\omega_{0nk}^2 - \omega^2)^2 + 4\alpha_{nk}^2 \omega^2}}, \quad \tan\theta'_{nk} = \frac{B'_{nk}(\omega_{0nk}^2 - \omega^2) - 2\alpha_{nk} \omega A'_{nk}}{A'_{nk}(\omega_{0nk}^2 - \omega^2) + 2\alpha_{nk} \omega B'_{nk}}.$$

Similarly, the solution of the ordinary differential equation (2.5b), that corresponds to the case of no viscosity, is the sum of the general and particular solutions (2.8b) and (2.9b); however, in this case it is impossible to find the eigenvalues analytically since they must satisfy the algebraic equation of the third

degree. In this case, it can be easily shown that the real parts of all three eigenvalues are negative. Thus, equation (2.5b) has no unbounded time-increasing solutions

$$T_{nk,\text{cond}}^{\text{gen}}(t) = D_{1nk}'' e^{\lambda_1 t} + D_{2nk}'' e^{\lambda_2 t} + D_{3nk}'' e^{\lambda_3 t}, \quad \lambda_i = (\lambda_x)_i + i(\lambda_y)_i, \quad (\lambda_x)_i < 0, \quad i = 1,2,3, \tag{2.8b}$$

$$T_{nk,\text{cond}}^{\text{part}}(t) = \Psi_{nk}'' \sin(\omega t + \theta_{nk}'') + \frac{C_{nk}''}{\beta_{nk}\omega_{0nk}^2}, \tag{2.9b}$$

$$\Psi_{nk}'' = \frac{\sqrt{A_{nk}''^2 + B_{nk}''^2}}{\sqrt{\beta_{nk}^2(\omega_{0nk}^2 - \gamma\omega^2)^2 + \omega^2(\omega_{0nk}^2 - \omega^2)^2}}, \quad \tan\theta_{nk} = \frac{B_{nk}\beta_{nk}(\omega_{0nk}^2 - \gamma\omega^2) - A_{nk}\omega(\omega_{0nk}^2 - \omega^2)}{A_{nk}\beta_{nk}(\omega_{0nk}^2 - \gamma\omega^2) + B_{nk}\omega(\omega_{0nk}^2 - \omega^2)}.$$

The unknown constants D_{ink}', $i = 1,2$ in the general solution (2.8a) and D_{ink}'', $i = 1,2,3$ in the solution (2.8b) can in principle be found from the initial conditions (2.7). After this, expressions (2.8) and (2.9) give the final solution of the original initial boundary-value problem (2.2)−(2.4). More interesting is the determination of the resonance conditions, namely, the conditions under which the amplitudes of the partial solutions (2.9) $\Psi_{nk}' = \Psi_{nk}^{\text{vis}}$ and $\Psi_{nk}'' = \Psi_{nk}^{\text{cond}}$ reach a maximum.

In the case of a viscous but non-thermal-conducting fluid, the resonance frequency can be obtained analytically. Differentiating the function $\Psi_{nk}^{\text{vis}}(\omega^2)$, we can show that the highest amplitude of the particular solution (2.9a) is achieved when

$$\omega_{\text{res}}^{\text{vis}} = \frac{3a_0^2}{4\nu_0}\sqrt{\sqrt{1 + \frac{32\nu_0^2}{9a_0^2}\left(\left(\frac{\pi n}{l}\right)^2 + \left(\frac{\pi k}{L}\right)^2\right)} - 1}. \tag{2.10}$$

In the case of an inviscid but heat-conducting fluid, differentiating the function $\Psi_{nk}^{\text{cond}}(\omega^2)$, we can show that the square of the resonance frequency $(\omega_{\text{res}}^{\text{cond}})^2$ must satisfy a fourth-degree algebraic equation (due to cumbersomeness, the equation is omitted). The search for the roots of this equation was carried out numerically.

In the case of the absence of viscosity and thermal conductivity (ideal fluid), the expression for the resonance frequency is noticeably simplified

$$\omega_{\text{res}}^{\text{ideal}} = \omega_{nk}^0 = a_0\sqrt{\left(\frac{\pi n}{l}\right)^2 + \left(\frac{\pi k}{L}\right)^2}. \tag{2.11}$$

However, in this case the behavior of the particular solution changes significantly, namely, it begins to grow indefinitely with time:

$$T_{nk,\text{ideal}}^{\text{part}}(t) = -\frac{A_{nk}'}{2\omega_{0nk}} t \cos(\omega_{0nk}t) + \frac{C_{nk}'}{\omega_{0nk}^2}.$$

We will analyze the obtained solutions for air. We take the length of the section equal to the channel length. The most important conclusion is that the "viscous" (2.10) and "heat-conducting" resonance frequencies differ from the corresponding frequency (2.11) for an ideal fluid by less than a hundredth of a percent. However, despite the practical coincidence of all three frequencies, there is a significant difference in the behavior of the corresponding solutions, namely, in the case of an ideal fluid, the highest amplitude tends to infinity. At the same time, the presence of dissipative effects (viscosity or thermal conductivity) leads to the fact that the highest amplitude immediately becomes finite. An analysis shows that the most dangerous (leading) frequency is the frequency $(\omega_{\text{res}}^{\text{lead}})_{11}$ that corresponds to the first harmonic $n = k = 1$. For the higher harmonics, the amplitude strengthening drops exponentially. Thus, the resonance is possible only at the first few frequencies.

In Fig. 2 we have plotted the graphs of the general solution (density) as a function of the longitudinal coordinate x at $y = 0.05$ m at the instant $t = 0.2$ s in the viscous non-heat-conducting case at various frequencies from the resonance spectrum. It can be seen that the density reaches its maximum amplitude at the leading frequency ω_{11}^{res}. On the other hand, the solution at the even frequency ω_{22}^{res} experiences minimal oscillations that are imperceptible for the chosen scale.
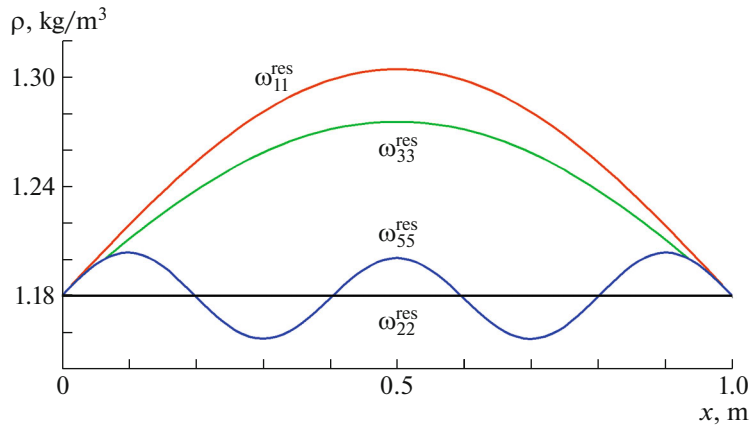
Fig. 2. Density as a function of the coordinate x in the viscous non-heat-conducting case at $y = 0.05$ m and $t = 0.2$ s for various particles of the resonance spectrum.

3. NUMERICAL SIMULATION

We will now go over to numerical solution to the original nonlinear system of equations (1.1)−(1.8) of the motion of a viscous compressible heat-conducting gas in the full geometry of a channel with five oscillating sections (Fig. 1a). The main method of integration will be *the method of separation by physical processes* [10]. Time integration is divided into two stages, namely, at the first (inviscid) stage, equations (1.1)−(1.6) are solved by neglecting the viscosity and thermal conductivity and, at the second stage, the effect of these dissipative terms on the parameters calculated at the first stage is taken into account.

In the absence of viscosity and thermal conductivity, system (1.1)−(1.6) is reduced to the gas dynamics equations. To solve them, a different type of splitting method was used − splitting along directions − the first stage of integration was also divided into two intermediate substeps. At the first substep, in the gas dynamics equations we retained the terms containing the derivatives only with respect to the coordinate x, and at the second substep the derivatives only with respect to the coordinate y. The resulting equations were solved using explicit schemes of the first order of accuracy, based on representation of the equations in the characteristic form and eliminating possible numerical oscillations.

At the second stage, the effect of viscosity and thermal conductivity on the parameters calculated at the first stage was considered. Finite-difference analogs of the resulting equations were written using ordinary implicit schemes of the second order of accuracy, to which the sweep method for tridiagonal matrices along the axis y is applied. The differences for various equations are only in the boundary conditions on the walls.

The computational area (rectangular channel) $\Omega = [0; \Lambda] \times [0; l]$ was divided into rectangular cells: four hundred cells in the direction x ($N_x = 400$) and two hundred in the direction y ($N_y = 200$). Initially, the channel is occupied by a fluid at rest, the pressure and the temperature are constant. At the initial instant $t = 0$, the pressure rises at the inlet and the walls begin to oscillate at the same time.

It is important to note that the walls are at rest in all calculations, and their influence on the flow goes through the boundary conditions (1.7a) and (1.7b). As a justification for this approach, we can say that the real motion of the walls (oscillations) covers a smaller distance than the width of one cell.

As the test problems, we considered the stationary Couette flow of a viscous compressible heat-conducting fluid and the unsteady Poiseuille flow of an incompressible and non-heat-conducting fluid. Under the usual assumptions, both problems admit analytical solutions. For all problems, a good agreement between the numerical and analytical results was obtained, namely, the error was less than one percent. Grid convergence was also studied. Both test problems were calculated on the coarse ($N_x = 300$, $N_y = 175$) and condensed ($N_x = 500$, $N_y = 225$) grids. The distributions of the main parameters (velocity and temperature) differed by less than one percent. The resonance condition (2.11) turned out to be insensitive to the particular type of grid.

We will now go over to the results of flow calculations in a channel with oscillating sections. All five sections have the same length $L = 0.1$ m, the channel length $\Lambda = 1$ m and width $l = 0.1$ m. As a working fluid (gas), we use a gas that is five times more viscous than air. The stationary regime of the flow under
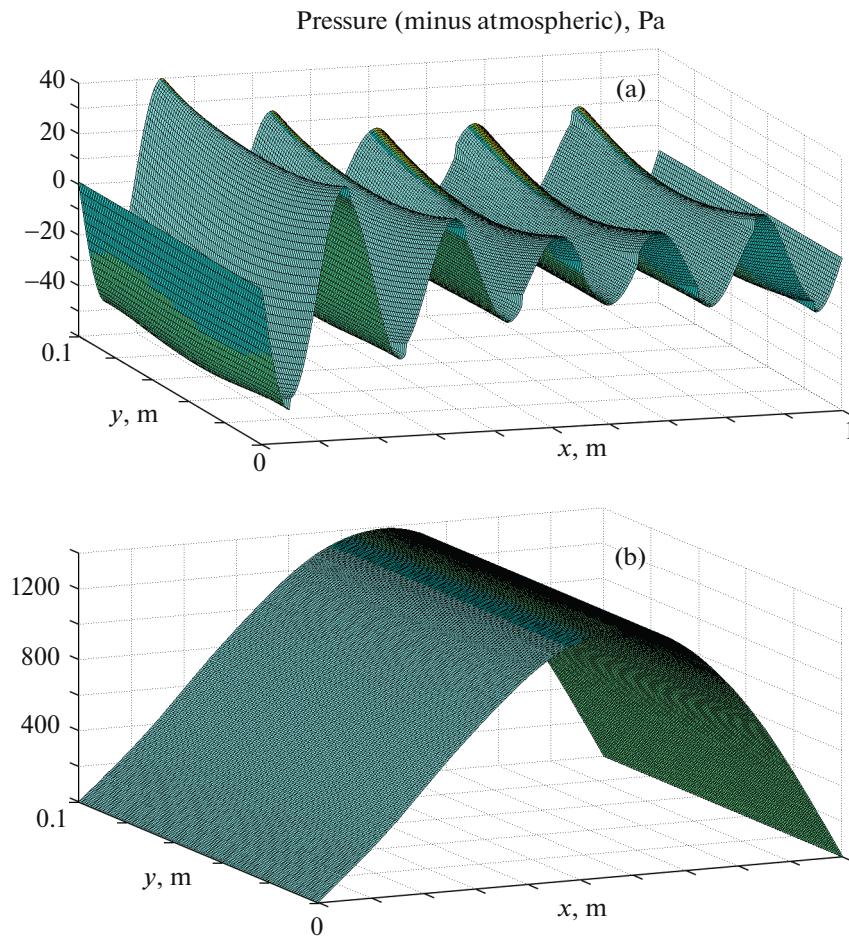
Pressure (minus atmospheric), Pa

Fig. 3. Pressure distribution in a channel with five oscillating sections at $t = 40$ s: (a) wall oscillations do not lead to the cumulative resonance, the frequency ω_{11}^{res}; (b) wall oscillations give rise to the cumulative resonance at the leading frequency ω_{01}^{res}.

the considered conditions occurs in about 60 s. The importance of reaching the stationary regime is as follows: we must clearly show that the cumulative resonance effect (growth) of the flow rate in the steady state in the presence of oscillating sections is significantly greater than the steady flow rate in the channel with the walls at rest.

The key dimensionless parameters of the calculations will be the vibrational Reynolds number and the Mach number. The Mach numbers will be extremely small M ~ 0.1, but the vibrational Reynolds numbers that correspond to the resonance regimes turn out to be fairly large $\alpha \sim 1.5 \times 10^5$. The main dimensional parameter describing the flow will be the mass flow rate of the working gas Q. The outlet cross-section of the channel was chosen as the control cross-section. The pressure at the channel outlet always remains atmospheric.

Note that the simplified analytical formulation of Section 2, in which the boundary conditions (2.3) of the first kind (of the Dirichlet type) are homogeneous only for the density, leads to the fact that the onset of resonance is possible at the leading frequency $n = 1$, $k = 1$. However, the complete nonlinear formulation includes non-uniform boundary conditions of the first and second kind (of the Neumann type) for various parameters (pressure, longitudinal velocity, and temperature). As a result, in the calculations the onset of resonance becomes possible at the lower frequencies: $n = 1$, $k = 0$ and $n = 0$, $k = 1$.

In all the calculations carried out, the resonance occurred at a frequency corresponding to $n = 0$, $k = 1$, because this frequency turned out to be the lowest one $\omega_{01}^{res} = 1089$ Hz. Note that this value seems to be quite realistic for technical applications. Amplification of the amplitude at this frequency (we will call it
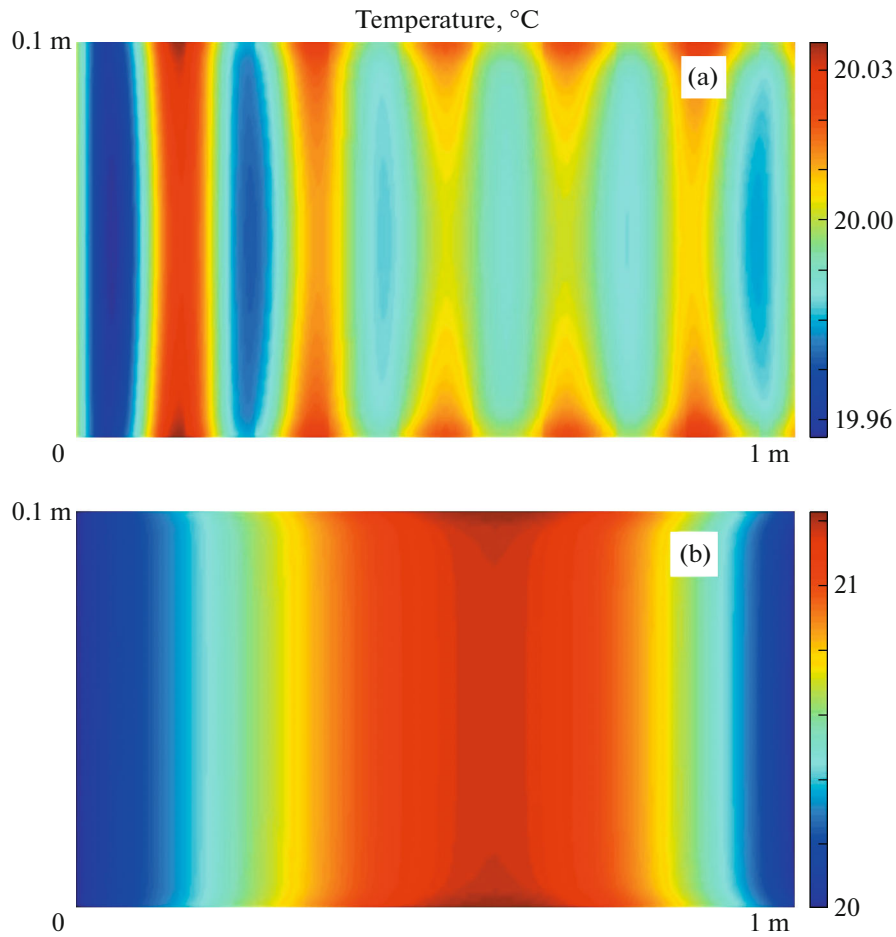
Fig. 4. Temperature distribution in a channel with five oscillating sections at $t = 40\,\text{s}$: (a) wall oscillations do not lead to the cumulative resonance, the frequency ω_{11}^{res}; (b) wall oscillations give rise to the cumulative resonance at the leading frequency ω_{01}^{res}.

the leading frequency) turned out to be the most intense. In addition, the cumulative resonance (after some time) was observed only at the leading frequency ω_{01}^{res}.

In the presence of oscillating sections, all flow parameters begin to vary periodically together with oscillations. However, the greater the difference between the wall oscillation frequency and the resonance frequency, the smaller the amplitude of these parameter oscillations. In Figs. 3 and 4 we have demonstrated the behavior of the pressure and the temperature in the normal and resonant regimes at the instant $t = 40$ s. The upper and lower sections oscillate at the same frequency in the in-phase operation. The maximum amplitude of the transverse velocity oscillations was $V_0 = 0.05$ m/s or approximately $10^{-2}U_0$.

In Figs. 3a and 4a the wall oscillations take place at a frequency from the resonant spectrum ω_{11}^{res} which does not lead to the cumulative effect. The periodic nature of the solution is clearly seen. In Figs. 3b and 4b the walls oscillate at the leading frequency ω_{01}^{res}. We can see a sharp increase in the pressure along the center of the channel, which corresponds to the results of the linear theory (Fig. 2). Fluid heats up towards the middle of the channel, but the changes in the temperature are no more than a degree.

Figure 5 shows the main result that demonstrates multiple increase in the mass flow rate. The cumulative resonance, i.e., sharp increase in the total mass flow rate (black curve), takes place only at the leading resonant frequency ω_{01}^{res} after some "steady" periodic variations in the pressure, the density, and the temperature. It can be seen that the cumulative resonance occurs only at the leading frequency approximately one minute after the start of oscillations. By this instant, for the channel with the walls at rest the
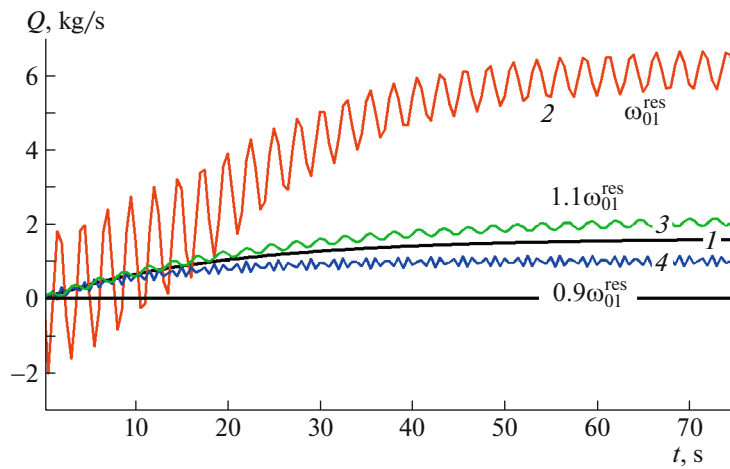
Fig. 5. Average mass flow rate at the channel outlet as a function of time: curve *1* corresponds to the walls at rest; curve *2* corresponds to the oscillations of sections at the leading resonant frequency; curves *3* and *4* correspond to the oscillations at the "near-resonance" frequencies.

flow rate has already reached the steady-state regime. In the near-resonance case $\omega = 1.1\omega_{01}^{res}$, the effect is already much smaller or completely absent at $\omega = 0.9\omega_{01}^{res}$. For the higher frequencies of the resonance spectrum ω_{10}^{res} and ω_{11}^{res} our calculations show that the difference is almost not observed as compared with the absence of oscillations.

Based on the results of variation in the mass flow rate, the entire process can be divided into three stages, namely, periodic variations in the main parameters in accordance with the vibrations of the walls, the cumulative nonlinear resonance, i.e., a sharp increase in the total mass flow rate, and the last stage — damping the oscillations due to viscosity and thermal conductivity, so that the mass flow rate gradually tends to a stationary value.

Note that even in the resonance regime the variations in temperature are negligibly small (half a degree). This does not lead to significant change in the viscosity and the thermal conductivity which remain practically constant. Thus, the cumulative effect of increase in the flow rate is a consequence of just the resonance effect.

SUMMARY

The main result of the study is the *cumulative resonance*, i.e., a significant increase in the mass flow rate of the fluid at a given constant pressure gradient. This effect is found on the basis of linearized solutions and numerical simulation. An exact analytical expression for the resonance frequency in a channel with oscillating walls is obtained in the case of an ideal (inviscid and non-heat-conducting) fluid. Accounting for viscosity and thermal conductivity leads to an insignificant (less than hundredths of a percent) change in the frequency. However, the amplitude of the solution becomes finite immediately.

It is shown that the resonance frequency is determined by the *geometry of the channel* (namely, its width and length), as well as by the *speed of sound* (that depends only on the temperature). The speed of sound is determined by the degree of compressibility of fluid. The resonance leads to periodic changes in the flow parameters with the maximum possible amplitude. Numerical calculations have shown that only five oscillating sections are sufficient for the cumulative effect to occur.

The main, but far from the only application of the results obtained is the flow of gas and oil in pipelines or water in piston pumps.

REFERENCES

1. Ganiev, O.R., Ganiev, R.F., Zvyagin, A.V., Ukrainskii, L.E., and Ustenko, I.G., Enhanced oil recovery based on the waveguide effects. Nonmonotonicity of damping of two-dimensional waves in a waveguide, *Spr. Inzh. Zhurn,* 2016, vol. 228, no. 3, pp. 42−48.

2. Ganiev, O.R., Ganiev, R.F., Zvyagin, A.V., Ukrainskii, L.E., and Ustenko, I.G., Enhanced oil recovery based on waveguide effects. Distribution of the force exerted on particles in the waveguide in a harmonic wave field, *Spr. Inzh. Zhurn,* 2016, vol. 229, no. 4, pp. 49−56.

3. Secomb, T.W., Flow in a channel with pulsating walls, *J. Fluid. Mech.*, 1978, vol. 88, pp. 273−288.

4. Hall, P. and Papageorgiou, D.T., The onset of chaos in a class of Navier−Stokes solutions, *J. Fluid. Mech.*, 1999, vol. 393, pp. 59−87.

5. Mingalev, S.V., Filippov, L.O., and Lyubimova, T.P., Flow rate in a channel with small-amplitude pulsating walls, *Euro. J. Mech. B/Fl.*, 2015, vol. 51, pp. 1−7.

6. Tukmakov, A.L., Gas flow in a plane channel with vibrating walls, *Inzh.-Fiz. Zh.*, 2002, vol. 75. no. 6, pp. 109−115.

7. Smirmov, N.N., Shugan, I.V., and Legros, J.C., Streaming flows in a channel with elastic walls, *Phys. Fluids*, 2002, vol. 14, no. 10, pp. 1−10.

8. Bagchi, S., Gupta, K., Kushari, A., and Iyengar, N.G.R., Experimental study of pressure fluctuations and flow perturbations in air flow through vibrating pipes, *J. Sound. Vibr.*, 2009, vol. 328, pp. 441−455.

9. Logvinov, O.A. and Malashin, A.A., Resonance phenomena in a channel with oscillating walls, *Euro. J. Mech. B/Fl.*, 2020, vol. 83, pp. 205−211.

10. Kovenya, V.M. and Yakovenko, N.N., *Metod rasshchepleniya peremennykh v zadachakh gazovoi dinamiki* (Variable Splitting Method in Gas Dynamics Problems), Novosibirsk: Nauka, 1981.

Translated by E.A. Pushkar